In Vitro Study of Coded Transmission in Synthetic Aperture Ultrasound Imaging Systems

Ihor Trots, Yuriy Tasinkevych, Andrzej Nowicki and Marcin Lewandowski

Abstract—In the paper the study of synthetic transmit aperture method applying the Golay coded transmission for medical ultrasound imaging is presented. Longer coded excitation allows to increase the total energy of the transmitted signal without increasing the peak pressure. Moreover signal-to-noise ratio and penetration depth are improved while maintaining high ultrasound image resolution. In the work the 128-element linear transducer array with 0.3 mm inter-element spacing excited by one cycle and the 8 and 16-bit Golay coded sequences at nominal frequency 4 MHz was used. To generate a spherical wave covering the full image region a single element transmission aperture was used and all the elements received the echo signals. The comparison of 2D ultrasound images of the tissue mimicking phantom and in vitro measurements of the beef liver is presented to illustrate the benefits of the coded transmission. The results were obtained using the synthetic aperture algorithm with transmit and receive signals correction based on a single element directivity function.

Keywords—Golay coded sequences, radiation pattern, signal processing, synthetic aperture, ultrasound imaging.

I. INTRODUCTION

ULTRASOUND imaging has become one of the primary techniques for medical imaging mainly due to its accessibility, non-ionizing radiation, and real-time display. To provide an accurate clinical interpretation the highest possible image quality is required. The most commonly used image quality measures are penetration depth, spatial resolution and image contrast. The penetration depth of the ultrasound image can be increased by applying longer signals and compressing them later on with the help of matched filter. The compressed signal is similar to that obtained using a single short pulse but with much higher amplitude. The spatial resolution of the ultrasound image can be improved by using the synthetic aperture (SA) method in which information is acquired simultaneously by small transmit-receive apertures placed in different positions and then used to reconstruct the full image from the collected data.

Several methods were proposed to form a synthetic aperture for ultrasonic imaging. In synthetic aperture focusing technique (SAFT) imaging, at each time only a single array element transmits a pulse and receives the echo signal [1, 2]. Multi-element synthetic aperture focusing (MSAF) is an alternate to SAFT [3].

A group of elements transmit and receive signals simultaneously, and transmit beam is unfocused to emulate a single element response. The acoustic power and the signal-to-noise ratio are increased as compared to SAFT where a single element is used. Synthetic transmit aperture method (STA) is an alternate to a conventional phased array [4]. At each time a single array element transmits an ultrasound pulse and all elements receive the echo signals. The advantage of this approach is that full dynamic focusing can be applied to both transmit and receive modes, giving the highest imaging quality. The STA is done by splitting transmit aperture into several sub-apertures [5, 6]. At each time one sub-aperture transmits an ultrasound pulse and all the elements receive the echo signals. In all this methods it is assumed that the transmit and receive elements are the point-like sources and the dynamical focusing is realized by finding the geometric distance from the transmitting element to the imaging point and back to the receiving element. But when the element size is comparable to the wavelength the influence of the element directivity on the wave field generation and reception become significant and if ignored might be a source of errors and noise artifacts in the resulting image. In this paper we endeavor to modify the STA algorithm in order to take into account the single element directivity to improve the quality of the resulting image. For this purpose the array element is modeled as a narrow strip transducer with a time harmonic uniform pressure distribution over its width for the far-field radiation pattern calculation. An analytical expression for the corresponding directivity function is available in [7].

The main objective of this work is to implement the STA method and to apply longer complementary Golay coded sequences which allows to increase of the transmitted energy, to improve the SNR and, as a result, the ultrasound image contrast.

The comparison of 2D ultrasound images of the tissue mimicking phantom as well as a beef liver pattern study in vitro is presented. The results show that using longer Golay coded sequences allows increasing penetration depth and image contrast maintaining spatial resolution.

II. SYNTHETIC TRANSMIT APERTURE ALGORITHM

As an alternate to the conventional phased array imaging technique a synthetic transmit aperture method [4] can be used. It provides for the full dynamic focusing both in transmit and receive modes yielding the highest imaging quality. In this method, a full aperture is synthesized by using multiple firings. On each firing, a single element acts as a transmitter and all

elements as receivers. To synthesize an *N*-element phased array in both transmit and receive modes $N \times N$ independent recordings are required. Conceptually, an STA system has all the characteristics of a conventional phased array. The depth of field is extended without any reduction in frame rate. The focusing is performed by finding the geometric distance from the transmitting element to the imaging point and back to the receiving element. The structure of the synthetic aperture and geometric relation between the transmit and receive element combination is shown in Fig. 1.
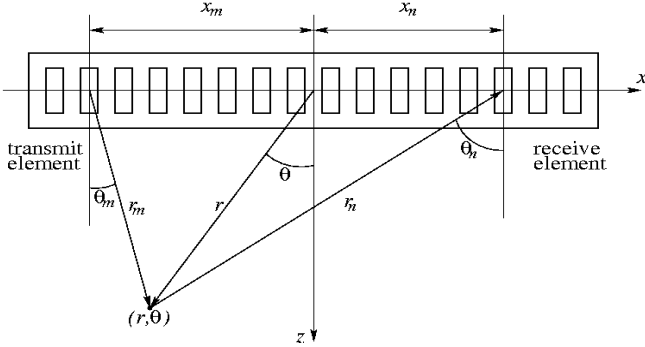

Fig. 1 Geometric relation between the transmit and receive element combination and the focal point

When a short pulse is transmitted by the element *m* and the echo signal is received by the element *n*, as shown in Fig.1, the round-trip delay is

$$\tau_{m,n} = \tau_m + \tau_n , \qquad (1)$$

where (m, n) is the transmit-receive element combination, $1 \leq m, n \leq N$. The corresponding delays for *m*'th and *n*'th element relative to the imaging point (r,θ) are

$$\tau_i = \frac{1}{c}\left(r - \sqrt{r^2 + x_i^2 - 2x_i r \sin\theta} \right), \quad i = m,n , \quad (2)$$

where x_m, x_n are the positions of the *m*'th and *n*'th elements, respectively, and r, θ are the polar coordinates of the imaging point (r, θ) with respect to the origin placed in the center of the transducer's aperture. In the case of the *N*-element array for each point in the image, the A-scan signal can be expressed as follows

$$A(r,\theta) = \sum_{m=1}^{N} \sum_{n=1}^{N} y_{m,n}\left(\frac{2r}{c} - \tau_{m,n} \right), \qquad (3)$$

where $y_{m,n}(t)$ is the echo signal and $\tau_{m,n}$ is the round-trip delay defined in (1) for the (m, n) transmit-receive element combination. The first and the second summations correspond to the transmit and receive beam-forming, respectively.

III. MODIFIED SYNTHETIC TRANSMIT APERTURE ALGORITHM

In the described above STA algorithm for each point in the resulting image every combination of transmit-receive pairs contributes according to the round-trip propagation time only.

The angular dependence is not taken into account in the applied point-like source model. But when the width of the array element is comparable to the wavelength corresponding to the nominal frequency of the emitted signal, the point-like source model becomes inaccurate. The element directivity influences the partial contribution to the resulting signal $A(r, \theta)$ in eq. (3) depending on the mutual position of the imaging point and transmit-receive pair, determined by the angles θ_m, θ_n (see Fig. 1). In this section a modified STA imaging algorithm which accounts for the element directivity function is developed and its influence on $A(r, \theta)$ is analysed. The underlying idea can be illustrated by the example shown in Fig. 2. In the case when the same element transmits and receives signal, the two scatterers located at the points with polar coordinates (r_i, θ_i), i=1,2 such that $r_{1m}=r_{2m}$ would contribute to the corresponding echo signal $y_{m,m}(t)$ simultaneously, since the round-trip propagation time $2r_{im}/c$, i=1,2 is the same. Apparently, the contribution from the scatterer at the point (r_1, θ_1) would be dominant, since the observation angle θ_{1m} coincides with the direction of maximum radiation for the *m*-th element, whereas its transmit-receive efficiency at the angle θ_{2m} is much smaller for the case of the scatterer at the point (r_2, θ_2). Thereby, evaluating the value of $A(r_2, \theta_2)$ from (3), the partial contribution of the echo $y_{m,m}(t)$ in addition to the correct signal from the obstacle located at (r_2, θ_2) (being small due to the large observation angle θ_{2m}), would also introduce the erroneous signal from the scatterer located at (r_1, θ_1). The latter signal is larger due to the small observation angle θ_{1m}. The larger observation angles appear in the imaging region close to the array aperture. Therefore, the most appreciable deviation from the point-like source model of the array element will occur there. A solution to the problem is proposed which accounts for the observation angle in accordance with the array element directivity function. Assume that the dependence of the transmit-receive efficiency of a single array element versus the observation angle is known and is denoted by $f(\theta_m)$, where θ_m is measured from the line parallel to *z*-axis and passing through the *m*-th element center. Thus, in order to suppress the erroneous influence from the scatterer located at (r_1, θ_1) on the value of the resulting signal $A(r_2, \theta_2)$, the partial contribution of the echo $y_{m,m}(t)$ is weighted by the corresponding value of $f(\theta_{2m})$. This corresponds to the superposed signal correction in accordance with respective contributions of individual scatterers located at the points (r_1, θ_1) and (r_2, θ_2).
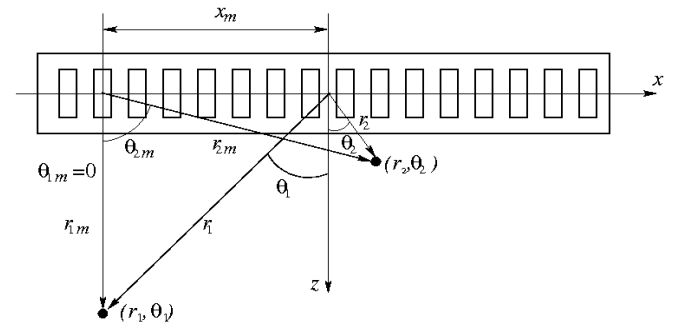

Fig. 2 Influence of the scatterer located at the point (r_1, θ_1) on the value of resulting signal $A(r_2, \theta_2)$ for imaging point (r_2, θ_2)

The above considerations lead to the following modification of the STA imaging algorithm

$$A(r,\theta) = \sum_{m=1}^{N} \sum_{n=1}^{N} f(\theta_m) f(\theta_n) y_{m,n} \left(\frac{2r}{c} - \tau_{m,n} \right), \quad (4)$$

where $\theta_i(r, \theta)$, $i=m,n$ are the corresponding observation angles for the transmit-receive pair. Note, that the angles depend on the spatial location of the imaging point (r, θ). The directivity function $f(\theta)$ can be calculated in the far-field approximation for a single element of the array transducer in analogous manner as in [7]

$$f(\theta) = \frac{\sin(\pi d / \lambda \sin \theta)}{\pi d / \lambda \sin \theta} \cos \theta, \quad (5)$$

where d is the element width, and λ is the wavelength. The above result applies to a narrow strip transducer with a time harmonic uniform pressure distribution along its width. It is obtained by means of the Rayleigh-Sommerfeld formula in the far-field region. The result is in a good agreement with experimental studies as shown by the authors in the cited work. For simplicity, we apply eq. (5) in the numerical results presented in the next section. It should be noted, that we use the angular response $f(\theta)$ in eq. (4) evaluated from eq. (5) for some fixed value of λ which corresponds to the nominal frequency of the transmitted signal. The far-field approximation is admissible for the case of STA algorithm discussed here. For the typical examples considered in the next section, the ratio $d/\lambda = 1.125$ is assumed. The far-field limit $r_{min} \approx 2d^2/\lambda$ [8] is 2.5λ, which requirement is met in the considered numerical experiments.

IV. GOLAY COMPLEMENTARY SEQUENCES

Ultrasound imaging allows to visualize structures and organs in real-time, enabling an instantaneously evaluation of clinical situation. But real problems appear when the reconstruction of the deeply located organs is needed. For that reason, coded excitation can be used making examination procedure more precise and allowing visualization of the deeply located organs in 2D B-mode ultrasound imaging.

Among the different excitation sequences proposed in ultrasonography, Golay codes evoke more and more interest in comparison with other signals. The reason of that lies in the fact that Golay codes, like no other signals, suppress to zero the amplitude of side-lobes. This type of complementary sequences has been introduced by Golay in the sixties [9]. In the seventies the Golay complementary codes were implemented using interdigital transducers accounting for the Doppler effect in surface acoustic waves (SAW) devices [10]. The pairs of Golay codes belong to a bigger family of signals, which consist of two binary sequences of the same length n, whose auto-correlation functions have the side-lobes equal in magnitude but opposite in sign. The sum of these auto-correlation functions gives a single auto-correlation function with the peak of $2n$ and zero elsewhere [11].

Fig. 3 shows the pair of complementary Golay sequences, their autocorrelations, and the zero side-lobes sum of their autocorrelations.
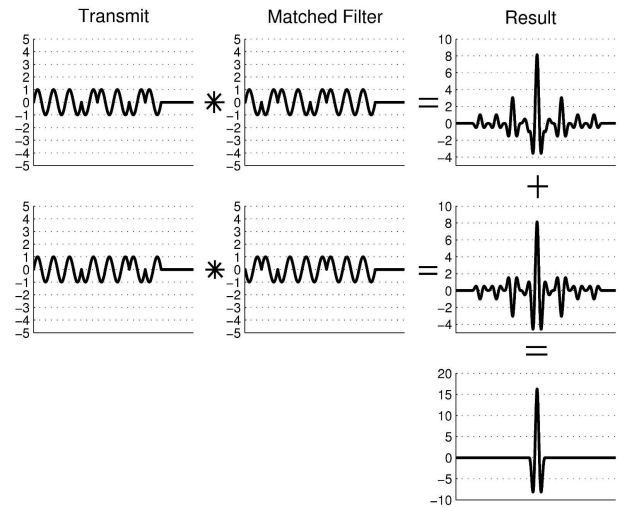

Fig. 3 Principle of side-lobes cancellation using pair of Golay complementary sequences of length 8 bits

V. COMPUTER SIMULATION

All simulations in this work are carried out with a powerful software, *Field II* [12]. The program is developed especially for investigating ultrasound fields, and gives the possibility to simulate and calculate ultrasound fields and defining one's own transducer. *Field II* is based on numerical analysis and runs under Matlab. The STA algorithm is used in the numerical examples presented in this paper. To simulate a measurement numerous parameters have to be set. The transducer used in the measurements described later is the linear transducer L14-5/38. The parameters used in the simulations are similar to those of the transducer. The medium in the simulations is homogenous and such parameters as the attenuation and the speed of sound were set to be the same as in experiments. The numerical results presented in Fig. 4 were performed for a 128-element linear transducer array with 0.3 mm pitch excited by one sine cycle burst pulse at a nominal frequency of 4 MHz. The element pitch is about λ, where λ corresponds to the nominal frequency of the burst pulse. The STA algorithm is employed. The transmit and receive elements combinations give a total of 128×128 possible RF A-lines. All these A-lines echo signals are sampled independently at a frequency of 40 MHz and stored in RAM.
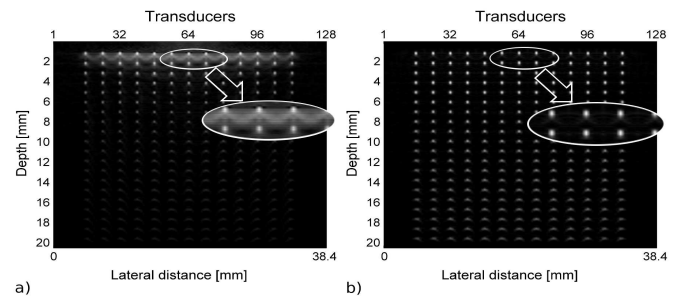

Fig. 4 Simulation of multi-point scatterers for 128-element linear array: a) not including directional diagram of element; b) including element directional diagram. Marked area is magnified evidencing suppression of the "noise"-like spatial variations of the scattered signal from the reflectors positioned near the transducer surface

The blurring of the scatterers placed near the aperture is significantly diminished in the case of introducing the directional diagram of element in synthetic focusing algorithm as compared to the algorithm without this correction

In Fig. 5 a computer simulation of multi-scatterers phantom when a 128-element linear transducer array was applied is shown. The one cycle as well as the pairs of complementary Golay sequences of the lengths 8 and 16 bits at nominal frequency 4 MHz were used. The phantom attenuation is equal to 0.5 dB/(MHz·cm). In the applied STA algorithm the element directivity correction scheme, discussed in [13], was implemented to improve the image quality near transducer aperture.
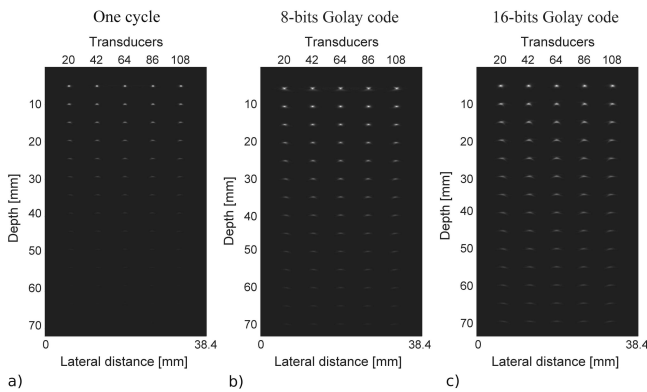

Fig. 5 Comparison of 2D ultrasound images obtained by computer simulation for 128-element linear array using: a) one cycle; b) 8-bit Golay sequences; c) 16-bit Golay sequences

The obtained 2D ultrasound images clearly demonstrate the advantage of using the Golay coded sequences. With the elongation of the coded sequences the acoustical energy increases yielding a higher SNR, that leads to an increase in the penetration depth while maintaining both axial and lateral resolution. The latter depends on transducer acoustic field and is discussed in [14]. The visualization depth when the one cycle was applied is equal to about 3 cm (Fig. 5a), while in case of applying 8-bit Golay codes this depth increases to 5 cm (Fig. 5b), and for longer 16-bit Golay codes this depth of visualization increases up to 7 cm (Fig. 5c).

In order to compare the lateral resolution the cross section of phantom at depths of 10 mm and 30 mm is shown in Fig. 6. Note, the normalization is performing with respect to the maximum values of the corresponding cross sections at different depth.

In Fig. 6 it can be seen that the lateral resolution at the different depths for all burst signals is the same. As anticipated, the lateral resolution illustrated in Fig. 6 as a function of depth is almost unchanged for the Golay codes of different length (being the function of the system bandwidth it is independent of the code duration [8].
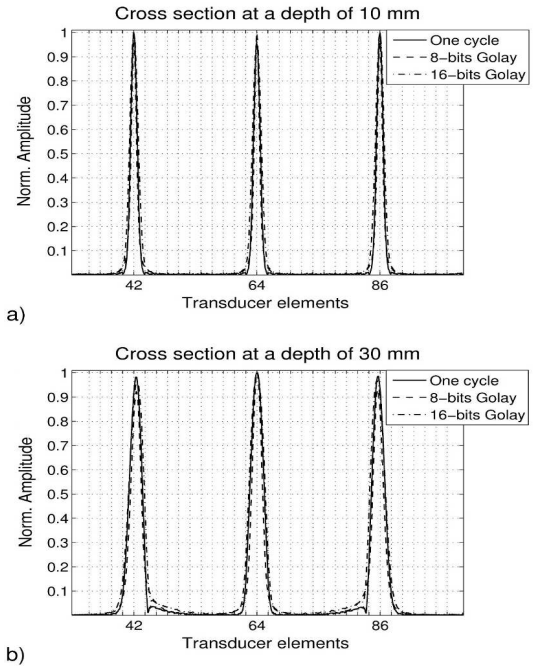

Fig. 6 Comparison of the lateral resolution at depths of 10 mm (a) and 30 mm (b) when one cycle, 8 and 16-bit Golay codes used

VI. EXPERIMENTAL RESULTS AND DISCUSSION

It's main part is an Ultrasonix - SonixTOUCH Research System (Ultrasonix Medical Corporation, Canada) equipped with a 128-element linear transducer array with 0.3 mm pitch. Ultrasonix enables a full control of transmission and reception parameters for all 128 elements of the transducer. Besides, a full access to raw RF data enables one to send it to the PC for further digital processing. Next, the processed data are displayed on the monitor. All post processing and display is done on PC using Matlab®. The processing creates 2D ultrasound image focused in every point.

The 128-element linear transducer array excited by the 8 and 16-bit Golay coded sequences as well as a one cycle at nominal frequencies 4 MHz were used in the experiments. A single element in the transducer transmitting aperture was used to generate an ultrasound wave covering the full image region. All elements were used for both transmitting and receiving. The RF echo signals sampled independently at 40 MHz and processed by the STA algorithm. Experimental data were acquired by an Ultrasonix - SonixTOUCH Research System (Ultrasonix Medical Corporation, Canada).

The tissue mimicking phantom model 525 Danish Phantom Design with attenuation of background material 0.5 dB/(MHz·cm) was used. It consists of several nylon filaments twists 0.1 mm in diameter positioned every 1 cm axially. This phantom allows to examine the axial and lateral resolution at various depths in the ultrasound image.

The comparison of the 2D ultrasound images of the tissue phantom obtained for one cycle, 8-bit and 16-bit Golay complementary sequences is shown in Fig. 8. The peak pressure level of excitation signals at the transducer were set as

low as possible to visually detect the echoes received using one cycle burst transmission slightly larger than the noise level. The same peak pressure has been used for the coded transmission.
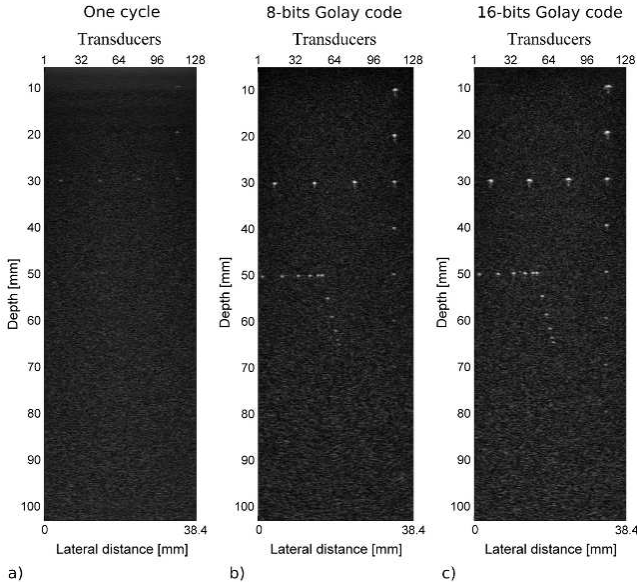

Fig. 8 2D ultrasound images of tissue mimicking phantom using: a) one cycle; b) 8-bit Golay code; c) 16-bit Golay code

The obtained 2D ultrasound images show an excellent performance of the coded excitation in terms of increasing penetration depth. In the case of one cycle the penetration depth is equal only to 3cm (Fig. 8a). In the case of 8-bit Golay code the penetration depth increases up to 7 cm (Fig. 8b). With the elongation of the coded sequences to 16 bits the acoustical energy increases yielding higher SNR, that leads to an increase in the penetration depth up to 8 cm (Fig. 8c). Note that axial and lateral resolution is the same for the all burst signals.

In order to compare quantitatively the SNR gain the 112th line from 128 RF-lines of the 2D ultrasound images is shown in Fig. 9 and the SNR is calculated. For this purpose the noise level which appeared straight after the signal was chosen.

Fig. 9 shows that applying coded transmission in comparison to one cycle pulse allows to improve the SNR by about 15 dB. Elongating the coded transmission twice leads to the SNR increase by about 1.4 dB which is in agreement with the studies shown in [7] where the final output is *2L* times larger (*L* is the coded length) than the response to a single impulse; however, the noise increases by a factor of $\sqrt{2L}$ ($\sqrt{L}$ for each correlation and $\sqrt{2}$ for the addition). Therefore, an improvement in the SNR of $\sqrt{2L}$ is obtained in comparison with the single period burst transmission. More realistically, for transmit two sequences per observation time, the SNR improvement factor is $\sqrt{L}$. The SNR increase in its turn leads to improvement of the penetration depth and the contrast of the image.
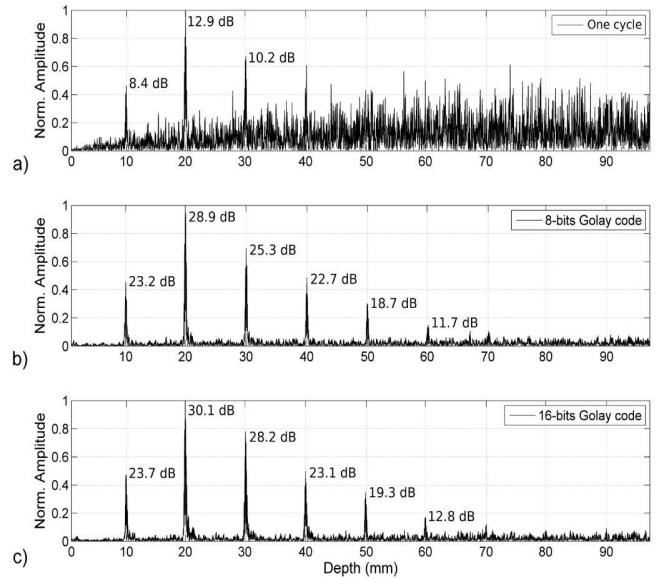

Fig. 9 The RF-lines of the tissue mimicking phantom using: a) one cycle; b) 8-bit Golay code; c) 16-bit Golay code

The comparison of 2D ultrasound images of beef liver pattern study in vitro for different burst signals are shown. Fresh beef liver sample was obtained from the local butcher shop within 6–8 hours after slaughter. It was refrigerated until being transferred to the lab. Ultrasonic experiments were conducted within 7-9 hours of the removal of the liver from the animal. The bovine liver sample was immersed in water at room temperature during the measurements.

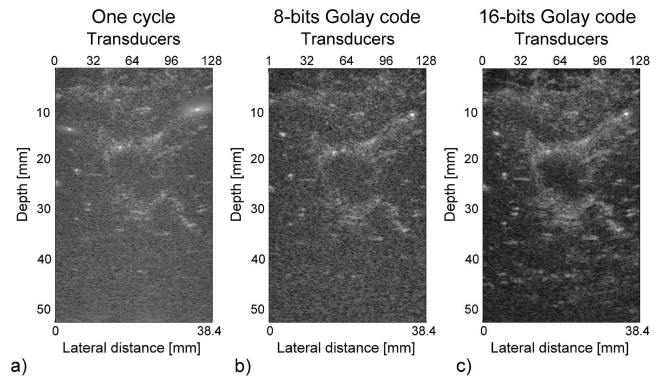The same peak pressure has been used for all signal bursts.

Fig. 10 2D ultrasound images of beef liver pattern study in vitro using: a) one cycle; b) 8-bit Golay code; c) 16-bit Golay code

As seen in Fig. 10 the air bubbles are observed which are almost impossible to avoid in case of in vitro experiments. But here they are helpful for qualitative estimation of the image quality parameters like the lateral resolution and contrast. At the same time the basic liver structure is unchanged in the presented experimental results. As expected, applying of the Golay coded transmission improves penetration depth and image contrast. The ultrasound penetration is nearly doubled for the 16-bit Golay codes in comparison with the single cycle transmission, effectively extending the diagnosable region in the practical medical application.

VII. CONCLUSION

The purpose of this work was to improve the penetration depth and the SNR in medical ultrasound imaging. To achieve the purpose the complementary Golay coded sequences were applied in the STA systems. The coded sequences were elongated from 8-bits to 16-bits which allowed to increase the penetration depth by about 2 cm. This is illustrated by the comparison of 2D images. The assumption that the application of coded transmission in the STA method in a standard ultrasound scanner could improve the penetration depth and image contrast has also been confirmed by the in vitro study of the beef liver pattern.

The new algorithm based on the array element angular directivity function has been introduced into the conventional STA method and the corresponding correction of the back-scattered RF-signals of different transmit-receive pairs has been made. It is shown that the far-field radiation pattern of a narrow strip transducer, calculated for the case of a time harmonic uniform pressure distribution over its width, can serve as a good approximation for the above directivity function. The results of numerical calculations using simulated data have shown distinguishable improvement of the imaging quality of the scatterers situated in the region near the transducer aperture, the hazy blurring artifacts, observable in the case of conventional STA algorithm, are substantially suppressed.

REFERENCES

[1] M. O'Donnell, L. J. Thomas, "Efficient synthetic aperture imaging from a circular aperture with possible application to catheter-based imaging," *IEEE Trans. Ultrason. Ferroelec. Freq. Contr.*, vol. 39, no. 3, pp. 366–380, 1992.

[2] R. N. Thomson, "Transverse and longitudinal resolution of the synthetic aperture focusing technique," *Ultrasonics*, vol. 22, no. 1, pp. 9–15, 1984.

[3] D. H. Johnson, D. E. Dudgeon, *Array Signal Processing: Concepts and Techniques*. Prentice-Hall, 1993.

[4] G. E. Trahey, L. F. Nock, "Synthetic receive aperture imaging with phase correction for motion and for tissue ihomogeneities — part I: Basic principles," *IEEE Trans. Ultrason. Ferroelec. Freq. Contr.*, vol. 39, no. 4, pp. 489–495, 1992.

[5] S. Holm, "Focused multi-element synthetic aperture imaging," Department of Informatics, University of Oslo, 1995.

[6] I. Trots, A. Nowicki, M. Lewandowski, "Synthetic transmit aperture in ultrasound imaging," *Archives of Acoustics*, vol. 34, no. 4, pp. 685 – 695, 2009.

[7] A. R. Selfridge, G. S. Kino, B. T. Khuri-Yakub, "A theory for the radiation pattern of a narrow-strip acoustic transducer," *Appl. Phys. Lett.*, vol. 37, no. 1, pp. 35-36, 1980.

[8] M. Xu, L.V. Wang, "Analytic explanation of spatial resolution related to bandwidth and detector aperture size in thermoacoustic or photoacoustic reconstruction," *Phys. Rev. E*, vol. 67, no. 5, pp. 1–15, 2003.

[9] M.J.E. Golay, "Complementary series," *IRE Tran. Inf. Theory*, vol. 7, pp. 82–87, 1961.

[10] E.J. Danicki, "Complementary code realization based on surface acoustic waves," *Bulletin of Military Technical Academy*, vol. XXIII, no. 1, pp. 53–56, 1974.

[11] I. Trots, A. Nowicki, W. Secomski, J. Litniewski, "Golay sequences – side-lobe canceling codes for ultrasonography," *Archives of Acoustics*, vol. 29, no. 1, pp. 87–97, 2004.

[12] J.A. Jensen, "Linear description of ultrasound imaging systems," *Note for the International Summer School on Advanced Ultrasound Imaging*, Technical University of Denmark, June 10, 1999.

[13] Y. Tasinkevych, I. Trots, A. Nowicki, P.A. Lewin, "Modified synthetic transmit aperture algorithm for ultrasound imaging," *Ultrasonics*, vol. 52, no. 2, pp. 333–342, 2012.

[14] A. Nowicki, Z. Klimonda, M. Lewandowski, J. Litniewski, P.A. Lewin, I. Trots, "Direct and post-compressed sound fields for different coded excitation," *Acoustical Imaging*, vol. 28, pp. 399–407, 2007.